TS

Figure 3- 2 Void Fractions calculated for the base case in terms of variation of the user-specific mixing diameter with respect to the corium jet diameter

TS

Figure 3- 3 Void Fractions calculated for the base case in terms of variation of the user-specific mixing diameter with respect to the corium jet diameter

TS

Figure 3- 4 Melt Fractions calculated for the base case in terms of variation of the user-specific mixing diameter with respect to the corium jet diameter

TS

Figure 3- 5 Void Fractions calculated for the base case in terms of variation of the user-specific mixing diameter with respect to the corium jet diameter

TS

Figure 3- 6 Pressures calculated for the base case in terms of variation of the user-specific mixing diameter with respect to the corium jet diameter

TS

Figure 3- 7 Void Fractions calculated for the base case in terms of variation of the user-specific mixing diamter with respect to the corium jet diameter

TS

Figure 3- 8 Impulses, Energy Transfer to Coolant, maximum Kinetic Energies of Coolant and the maximum Conversion Ratio calculated for the base case in terms of variation of the user-specific mixing diamter with respect to the corium jet diameter

TS

Figure 3- 9 Impulses and void fractions calculated for the base case in terms of variation of the user-specific mixing diamter with respect to the corium jet diameter

TS

Figure 3- 10 Models for the Reactor Case Analysis in the SERENA-I Project

TS

Figure 3- 11 Simplified steam explosion pressure profile for the structure analysis

TS

Figure 3- 12 Axisymmetric sketch of reactor vessel: (a) Geometry, (b) Grid and (c) Boundary Conditions

TS

Figure 3- 13 Results of Stress Analysis: (a) Von Mises Stress and (b) Equivalent Plastic Strain

TS

Figure 3- 14 Results for the maximum pressure of 50 MPa: (a) Maximum equivalent plastic strain, (b) Equivalent plastic strain at the maximum strain node, and (c) Von mises stress at the maximum strain node

TS

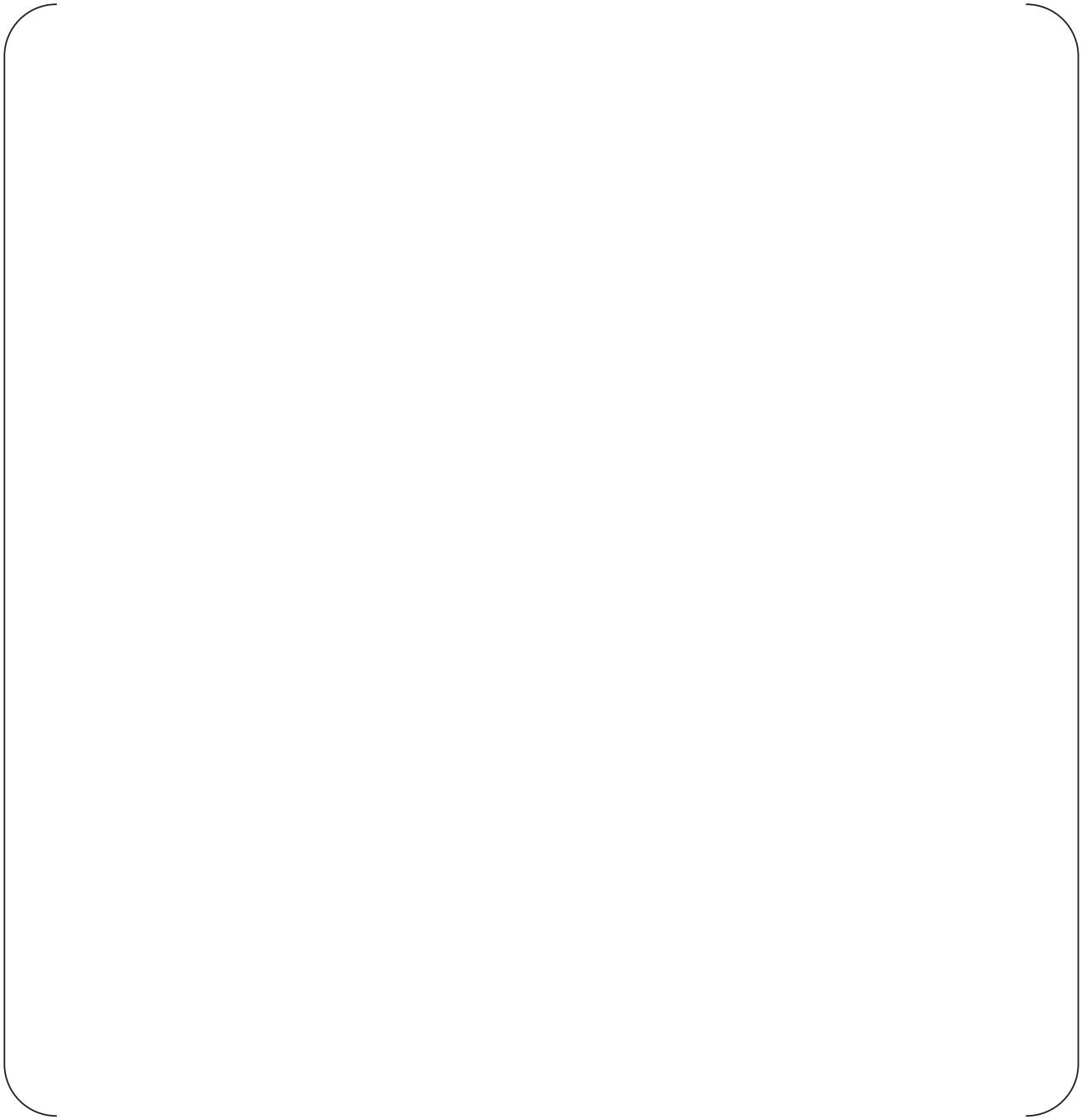

Figure 3- 15 Results for the maximum pressure of 100 MPa: (a) Maximum equivalent plastic strain, (b) Equivalent plastic strain at the maximum strain node, and (c) Von mises stress at the maximum strain node.

TS

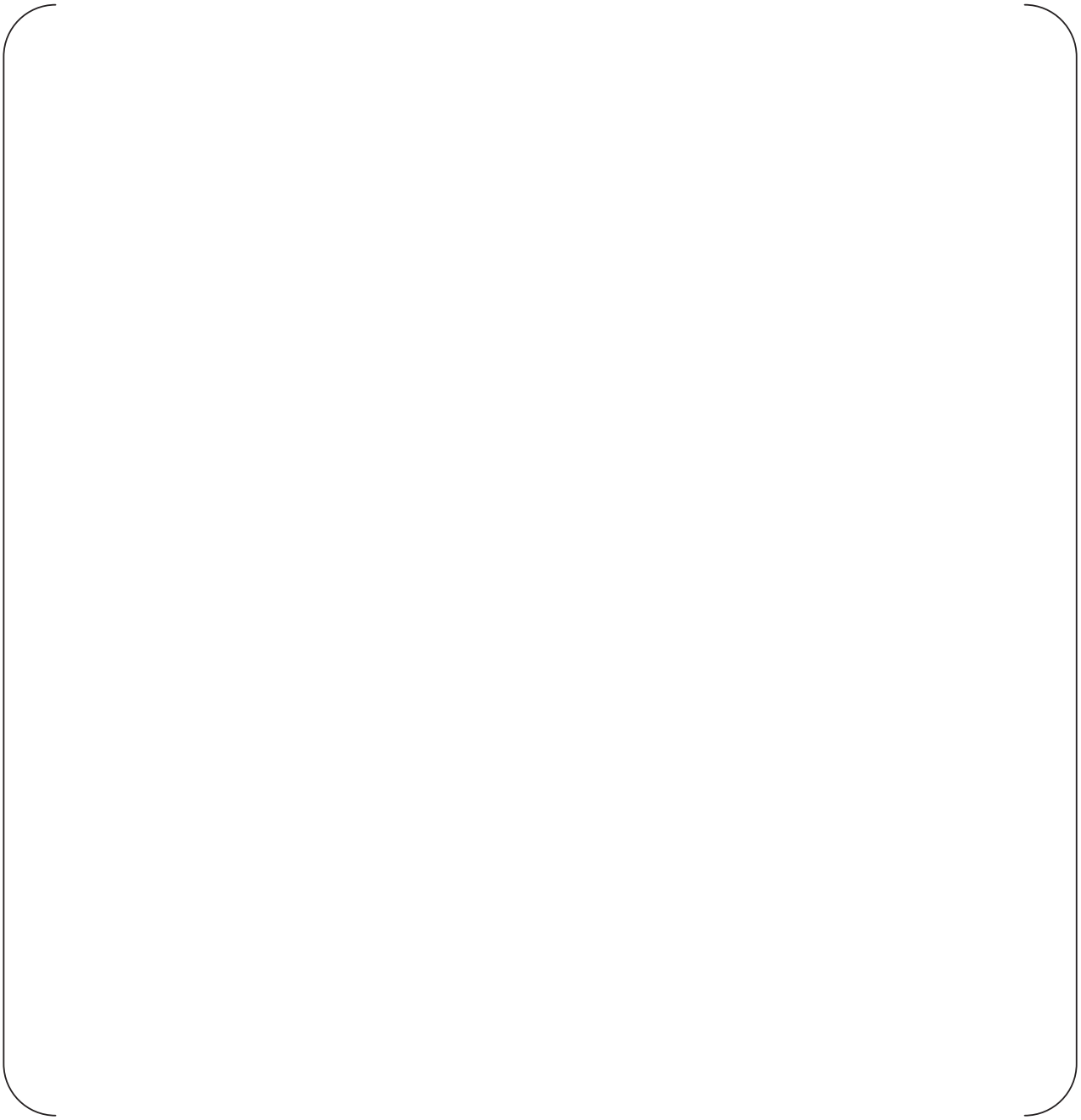

Figure 3- 16 Results for the maximum pressure of 150 MPa: (a) Maximum equivalent plastic strain, (b) Equivalent plastic strain at the maximum strain node, and (c) Von mises stress at the maximum strain node.

Figure 3- 17 Maximum hoop strain in terms of explosion impulse

TS

Figure 3- 18 Maximum plastic equivalent strains in terms of explosion impulse for the comparison with the failure criteria.

4.0 METHODOLOGIES OF STEAM EXPLOSION ANALYSIS FOR APR1400

4.1. Introductions

In this chapter, the APR1400 design specific analysis for the evaluation of ex-vessel steam explosion (EVSE) risk is discussed. The analysis consists of (a) determination of initial and boundary conditions for EVSE, (b) the evaluation of EVSE energetics, (c) the sensitivity analysis for key parameters that vary with the consideration of severe accident scenarios, measures and progression, and (d) finally, the analysis results is discussed to assess the EVSE risk in the APR1400 design.

4.2. Initial and Boundary Conditions of EVSE Analysis

In the EVSE analysis, it is of essence that vessel failure mode is identified to define the initial conditions of the EVSE analysis. However, the vessel failure mode is one of the most uncertain phenomena in the severe accidents since it requires understanding of the in-vessel severe accident progression as well as complex corium-vessel interaction. Therefore, the degree of uncertainty involved in the prediction of EVSE is determined by the sensitivity of those key uncertain parameters to the EVSE energetics. Minimizing the uncertainty associated with the determination of initial conditions for the EVSE analysis, the results from comprehensive system code analysis such as SCDAP/RELAP, MELCOR or MAAP in terms of risk-significant severe accident scenarios are often used. For instance, SCDAP/RELAP analysis for APR1400 plant [Reference 31] provides detailed quantitative prediction on the thermo-physical conditions of corium at vessel failure in terms of accident scenarios such as Total LOFW, SBO, and LOCA as shown in Table 4-1. In this analysis, the configuration of the melt components such as oxide and metal layers allows to evaluate the vessel failure location, corium composition, corium break velocity as well as the thermal conditions. However, the size of the vessel failure spot is still largely unknown although the size determines one of the most influential parameters, the corium jet diameter.

Recently, the MAAP analysis [Reference 32] is used to investigate the corium conditions when the reactor vessel fails for APR1400 plant considering several accident scenarios listed in Table 4-2. They employed MAAP4.0.8 to simulate a set of selected sequences in order to characterize the corium flow at vessel failure to provide initial conditions for ex-vessel steam explosion calculations as shown in Tables 4-3 to 4-5 for APR1400 design. The summary of the corium flow characteristics at vessel failure had been estimated in Table 4-6.

In this section, the initial and boundary conditions for the EVSE analysis will be determined by considering those analysis results as well as other experimental evidences.

In order to determine the initial and boundary conditions a few general assumptions related to FCI risk significant events of severe accident sequences are given below and further detailed assumptions for selecting a base case of the analysis are also given in the following sections.

- Ex-vessel steam explosion occurs at the partially flooded cavity with which the reactor pressure vessel is unable to be covered for ex-vessel cooling. This assumption was justified in the case of the complete station black-out event in when a passive cavity flooding is only available by opening a manual valve of the HVT tank connected to IRSWT. In the sensitivity analysis, the effects of the cavity water level on steam

explosion loadings are examined.

- The late in-vessel phase with a complete generation of a liquid corium pool in the RPV lower plenum is assumed. The internal corium pool thermal conditions at a vessel failure are provided by the SCDAP/RELAP-5 analysis [Reference 31, 43]

- Global RPV failure is assumed to be unphysical and thereby excluded when discharged corium from RPV is directly relocated to the flooded cavity without temporal accumulation near RPV.

- The main mode of vessel failure without adequate cooling mechanisms is assumed to be a side RPV break due to so-called focusing effect resulted from an overlying thick metallic corium layer. In the case, 100% metallic corium is assumed to be poured into a flooded cavity for steam explosions. In the sensitivity analysis, the bottom RPV failure with 100% oxide release through a break hole generated by a 2-4 ICI tubes.

4.2.1. Corium Characteristics

4.2.1.1. Corium composition and thermal properties

The reference corium composition 90%UO_2-10%ZrO_2 with its thermal and transport properties as shown in Table 3-1 is chosen as for the in-vessel steam explosion analysis. Table 4-7 indicates also the properties of corium composition of 80%UO_2-20%ZrO_2 that often used in experiments that most of thermo-physical properties are similar and no significant effects of those difference on the steam explosion energetics.

4.2.1.2. Corium temperature

The corium temperature of 3000 K that corresponds to the superheat of 150 K is selected for the base case EVSE analysis. In the MAAP analysis the mean corium temperature of 2705 K was obtained due to the complex composition of materials that lowers the melt eutectic temperature. However, it is important to note that the melt superheat of 151 K similar to other analyses, the SCDAP/RELAP 5 analysis [Reference 31, 5, 19]. For the AP1000 analysis [Reference 19], for instance, the oxidic layer corium temperature of 3150 K was used as a conservatively bounding case. In addition, it is difficult to use the MAAP analysis results on corium conditions (temperature, composition etc.) because the corium formed in the RPV lower head prior to vessel breach were assumed to be a mixture of oxide and metal components of corium. In this case, the corium temperature may be low due to the eutectic process as well as its properties may also differ from the oxide or the metal components that may form as separate layers during the corium relocation from reactor core to the RPV lower head. Therefore, the corium composition with the known thermo-physical properties (90%-10% corium) but with keeping the same corium melt superheat of 150 K suggested the initial corium temperature of 3000 K for this EVSE analysis. Since the corium temperature is one of the most significant parameters that influences to the EVSE energetics, sensitivity analyses cover the corium temperatures from 2900 (50 K superheat) up to 3150 K (300 K superheat).

For the metallic layer of the corium, there is a few analysis for reactor applications; the AP1000 analysis used the metallic corium temperature of 2060K. Therefore in this analysis, the ranges of

the metallic corium temperatures from 1700 up to 2300 K were chosen and the base case temperature of 2100K was selected.

4.2.2. Corium Discharge Characteristics

The reactor vessel failure will be inevitable consequence if a large molten corium pool generated in the lower plenum of the reactor vessel due to the corium relocation has no sufficient cooling from the vessel outside. Under the circumstances, the vessel steel experiences large degradation of its strength, resulting creep behavior due to the high temperature corium pool and pressure loading on the wall.

Some relevant information can be drawn from existing literatures [Reference 44, 45];

- Vessel steel creep accelerates when the wall temperature reaches more than 800 °C, much lower than corium melt pool temperature.
- The highest wall temperature on the vessel wall occurs at the location of the highest temperature of the melt pool established by a melt-pool convection.
- Molten corium pool produces multi-composition layer; top metallic layer, middle oxide layer and bottom metallic layer.
- Vessel failure experiments from the OECD-LHF and OLHF projects without a melt pool and the RIT-FOREVER with a melt pool shows a localized vessel failure at the hot spot of the wall temperature. In the FOREVER tests, the vessel failure always occurred at the hot spot, about 70° angle from the lower center of the vessel, on the wall produced by the melt pool convection.
- The creep rupture of the vessel occurs at a strain of 13~16% in the FOREVER test. It is worth to note that a vessel failure occurs at the location of the hot spot of the wall, not at the location of the largest strain or at the location of penetration which is usually located at near bottom of the vessel.
- Crack of the vessel similar to a fish mouth travels along the azimuthal direction to less than 30% of the vessel circumference.

Melt discharge rate due to the vessel failure depends on the vessel rupture characteristics originated from the vessel material properties. Amount of melt discharge due to a gradual rupture of the vessel results much less melt discharge than one with rapid rupture. Even in a moderate pressurized vessel (~ 20 bar), not all the melt was discharged at the time of failure.

4.2.2.1. Corium jet diameter (RPV Failure Size)

The vessel failure sizes depend largely on the thermo-mechanical interactions between the corium melt pool convections and the reactor vessel walls. Assuming no external cooling by cavity water is unavailable prior to the reactor vessel failure as a conservative ex-vessel scenario; the vessel failure is anticipated at the side of the vessel wall due to the focusing effect based upon the SCDAP/RELAP in-vessel analysis [Reference 31].

However, the estimation of vessel failure modes including the location, size and shape is hardly achievable in any certain degree. Based upon information above, the following postulations can be made for the estimation of a vessel breach size. This breach size will be considered as a corium jet diameter for the TEXAS analysis.

For the case of the side failure,

(a) the vessel fails at the interface at the top metallic layer,

(b) the global failure is remote,

(c) the crack shape of the vessel is a fish mouth

Under the assumptions, the maximum breach size can be obtained by assuming the breach hole diameter equal to the metallic melt layer thickness, ranging from 0.54-0.63m. The practical minimum size of the vessel breach size can be estimated by assuming the fish mouth failure observed in experiments and considered to be 0.1 m.

For the case of the bottom failure,

(a) localized failure of the 1-4 vessel penetration tubes is most likely and

(b) the global bottom rupture due to combined failure of adjacent penetration tubes are unlikely.

The MAAP analysis also suggested that RPV with penetration results mostly in the penetration failure than the creep rupture and the mean vessel failure diameter is suggested to 0.56 m with the standard deviation of 0.14m.

In general, h0wever, for the penetration failure, the vessel breach size, or the initial corium diameter, of 0.3 m is used [Reference 5] and the corium diameter of 0.5 m is used to represent the typical vessel failure size due to the creep rupture. In the MAAP analysis, no evidence of global vessel failure results in much larger corium jet diameter to be considered.

Based on the information, the initial corium diameter for the base case ex-vessel steam explosion is set to 0.3 m and the corium jet diameters from 0.1 to 0.6 m are considered for the sensitivity analysis.

4.2.2.2. Corium jet velocity

The corium jet velocity of 4 m/s is selected for the base case EVSE analysis considering the MAAP analysis results (see Table 4-8). For the sensitivity analysis, the initial corium jet velocities from 1 to 6 m/s were considered.

4.2.2.3. Water in Cavity

The cavity flooding system (CFS) is one of the main safety measures followed by the SAMG (Severe Accident Management Guideline) with which subcooled water floods the cavity and partially submerges the RPV as shown in Figure 4-1. The measure aims to prevent severe accidents

progression beyond in-vessel scenarios by providing ex-vessel cooling. In the case of failing in-vessel retention of corium, the flooded cavity provides long-term cooling of corium debris discharged from the failed RPV.

4.2.2.4. Containment ambient pressure

The containment ambient pressure increases during the severe accident progress. Typical 0.2 MPa containment pressure is selected. In general, since the effect of the ambient pressure in the ranges of order of few bars has little effect on the steam explosion energetics, the sensitivity analysis for this parameter is not considered.

4.2.2.5. Cavity water level

The CFS provides water from the IRSWT in two separate operations; (a) passive flooding by manual opening of HVT valves and (b) active flooding by operating External Reactor Vessel Cooling System. The first passive flooding operation fills water up to 6.4 m from the cavity floor within 1350 s from the HVT valve opening and the second active operation floods water up to 13.2 m for additional 2400 to 3000 s, covering approximately a half of RPV for ex-vessel cooling. The present base case analysis considered the risk of steam explosions as the IVR/ERVC measure is not provided. However, in the sensitivity analysis, fully flooded cavity water level that covers the RPV lower head to provide the IVR/ERVC measure is considered.

4.2.2.6. Cavity water subcooling

The water subcooling in the cavity is selected from the various analysis results to be ranged from 20 to 90 K at the estimated containment pressure, considering various analyses for the ex-vessel steam explosions. The base case condition of 42 K subcooling is selected by the consideration of the lower subcooling of coolant estimated by the MAAP analysis. However, the sensitivity analysis is performed for the subcooling ranges.

4.2.3. Summary

In summary, Table 4-8 lists the initial and boundary conditions for the base case of EVSE analysis and their minimum and maximum ranges. The base case is assumed to be the EVSE due to the bottom vessel failure with the partially flooded cavity. The side vessel failure case can be considered as a sensitivity study if the vessel failure occurs due to the focusing effect.

4.3. TEXAS-V Modeling

4.3.1. Nodalization

The plant geometry for the TEXAS-V analysis is shown in Figure 4-2(a). The computational nodalization for the TEXAS analysis for the RPV is built as shown in Figure 4-2(b).

The first nodalization group that represents the RPV water has 16 nodes that have the thickness of 0.4 m. The second nasalization that represents the gas buffer region has 12 nodes with the same node thickness of 0.4 m, because of the consideration of water level swelling during the mixing phase. Lastly, the third nasalization has seven nodes with the thickness of 1 m. The location of corium introduction is at 6.5 m. At the bottom of the nodes, trigger cell is located to provide the

trigger pressure. The diameter of the first and second nodes are the user input parameter, ARIY, that should be determined to let the 1-D TEXAS-V code produce the maximum energetics for given initial and boundary conditions. The diameter of the gas buffer zone is set for 50 m^2 sufficiently large.

4.4. Evaluation of Dynamic Loads of EVSE – Base Case

4.4.1. Mixing Phase of EVSE

Figure 4-3 illustrate the void fraction generated by corium jet penetration into cavity water during the mixing phase of the base case. The corium reached to the bottom of the RPV about 1.4 s when the explosion starts. The corium jet penetrates and breaks up into small particles. Figure 4-3 shows typical void generation where the larger amount of vapor void on the top of the cavity water, reaching up to 2% average void fraction. Figure 4-4 shows the fraction of melt along the axial direction in the cavity water. The void fractions in the lower region were very low although the corium jet fragmented. Therefore, it is expected that steam explosion can likely occur at the bottom and propagates upward, triggering subsequent explosions.

4.4.2. Explosion Phase of EVSE

Figures 4.5 and 4.8(a) show the steam explosion pressure profiles in terms of the explosion time. The maximum pressure and impulse of 60.519 MPa and 179.93 kPa-s, respectively. The pressure profiles show the typical shock characteristics as the rapid build-up of pressure front and a long tail with respect to time. The explosion pressure front traveled up and dissipated in the upper axial location due to the presence of a volume of steam as shown in the mixing phase.

Figures 4.6 shows the void fraction profiles during the explosion phase. The lower part of the lower head where steam explosion was triggered builds up steam due to the explosion during the period the explosion phase. The upper region however where the steam generated in the mixing phase shows the rapid condensation during the explosion phase period, 20 ms.

The impulse asserted to the surrounding structure was estimated by the integration of the explosion shock pressure during the explosion period. The evaluated impulses at each node are shown in Figure 4-7(a). The impulse at the node of cavity floor reached 179.93 kPa-s. The maximum possible energetics of steam explosion in this case estimated by the 1-D TEXAS-V analysis will travel (and be attenuated) to the surrounding cavity structure. The dissipation of shock pressure from a mixing zone to the cavity walls along the single phase cavity water is discussed in the next section. Figure 4-9 show the top view of the cavity structure. In this figure, seven locations at the cavity wall to evaluate the explosion shock attenuation at those cavity wall surface. The distances from the RPV center to the seven locations ranges from 2.159 to 5.744 m.

Figures 4.7(b), (c) and (d) show more insights of the explosion phase of the steam explosions in RPV that include the energy partitioning, the coolant kinetic energy and the conversion ratio history during the explosion phase. In particular, the conversion ratio of the steam explosion reaches its maximum of near 1.8% after the triggering of explosion.

4.4.2.1. Evaluation of Dynamic Loads of EVSE at the Cavity Walls

Shock pressure generated from the steam explosion in the reactor cavity pool propagates. In the

TEXAS code, however, due to its one-dimensionality of computational domain, the pressure generated at one location, x(z), can be tractable only in the vertical z-direction. Therefore, the impulse acts to the cavity wall in the radial direction requires additional analysis. The most recent version of the TEXAS-V code encompassed with the ANSYS CFD packages to analyze the radial shock propagation. On the other hand, the underwater shock propagation studied by Cole [Reference 46] known as a TNT method has been well applied for this purpose.

Figure 4-9 illustrates the reactor cavity arrangement in the APR1400 plant. The distances from the center axis of the RPV centerline to the near cavity walls are listed in Table 4-11. It is noted that the closest wall from the center has a distance of 2.159 m.

If the maximum explosion pressure at a known distance, for instance, $r=R_{mix}$, is ΔP_{mix}, the distance-dependent maximum explosion pressure, $\Delta P_m(r)$ becomes,

$$\Delta P_m = \Delta P_{max} \left(\frac{1}{r}\right)^{\alpha} \quad \text{(Eq. 4.1)}$$

where, α=1.13 and all units are the British units, ie., P [psia] and r [ft]. For instance, in the TEXAS-V analysis, it is difficult to evaluate the exact mixing zone for the steam explosion although the one-dimensional characteristic parameter, ARIY, was at to 7 m^2 that is the diameter of approximately 3 m. By assuming this diameter be the mixing zone and considering the distance from the outer mixing boundary to the near cavity wall, the maximum pressure propagation along the lateral direction to the cavity wall can be estimated by Eq. (4.1) using ΔP_{max}=60.51 MPa. Table 4-11 shows the estimated maximum pressures at the cavity walls that significantly attenuated from the EVSE maximum pressure. These estimated values can be used for the structure analysis of cavity integrity due to the EVSE loadings.

4.5. Sensitivity Study

For the sensitivity study, additional cases for issues associated with (a) vessel failure modes such as bottom failure due to penetration tube failure, and side vessel failure due to metallic layer focusing effect, (b) severe accident management strategies, and (c) key corium characteristics including the corium temperature, the velocity and diameter and the cavity water temperature are examined. Tables 4-12 to 16 show the result of the analyses in comparison to the base case. The details are discussed in the following sub-sections.

4.5.1. Reactor Vessel Failure Mode Issues

4.5.1.1. Side Vessel failure (SVF)

For the side vessel failure, the vessel failure location and break size are important parameters that determine the energetics of EVSE because it determines the mass of corium participated during EVSE and the distance between the mixing zone of steam explosion and the nearest cavity wall. In the case of a potential vessel failure due to the metallic corium layer focusing effect with assumption of the side vessel failure without IVR-ERVC (In-Vessel Core Melt Retention-External Reactor Vessel Cooling) SAM strategy, RPV is exposed to atmosphere and the location of side vessel failure occurs at 8.05 m above the cavity floor (~ 80^{O}) as shown in Figure 4-2(A).

The analysis shows that the peak pressure and corresponding impulse of 60.35 MPa and 194.07 kPa-s, as shown in Table 4-14, are estimated. The results are similar to those from the base case. As described in Table 4-8, the initial conditions for the SVF case assume that the corium is 100% metallic composition with high superheat of corium but lower temperature. In addition, the corium injection velocity at the vessel breach location is low due to the small gravitational head of corium in the reactor vessel. Comparing to the base case, the peak pressure due to steam explosion is similar but the impulse generated by the steam explosion is higher. The steam explosion loadings to the cavity wall will be higher than that of the base case due to the location of the vessel failure.

4.5.2. SAMG Related Issues: In-Vessel Corium Melt Retention (IVR)

For the case of IVR/ERVC, the RPV is in a stage of submersion in the fully flooded cavity water up to EL114'-4" from the plant ground level, or 13.8 m from the plant cavity floor (see Figure 4-2), to provide the external cooling when the core meltdown and relocation to the bottom of the reactor vessel occurs. In this situation, there is two potential vessel failure modes; bottom and side vessel failures at the locations assumed to be 6.5 and 8.05 m, respectively.

Table 4-12 shows that the peak pressures and maximum impulses for both bottom and side vessel failures with IVR-ERVC are 69.79 MPa, 217.33 kPa-s and 48.84 MPa, 226.16 kPa-s. It is noted that for the bottom vessel failure in the case of fully-flooded (FF) case, the explosion peak pressure is slightly higher but the impulse becomes about 20% higher. For the side vessel failure, however, it was observed that the tendency of explosion pressure profile was opposite to one for the bottom vessel failure, resulting in about 20% lower peak pressure but 26% higher impulse. The result indicates that the energetics of the side vessel failure is slightly higher than one of the bottom vessel failure.

4.5.3. Effects of Key Physical Parameters on EVSE Energetics

In this sensitivity analysis, some of key parameters pertaining to the thermal and dynamic properties of corium and the conditions of cavity water are examined to investigate their uncertainties on the energetics of EVSE in the APR1400 design. In this sensitivity analysis, it is worth to note that the mixing area defined by the model parameter, ARYI value of 7 m^2, is maintained in most of cases (except corium jet diameter effects).

4.5.3.1. Corium Temperature Effects

The effect of the initial corium temperatures on the EVSE energetics with the minimum and the maximum temperatures of 2900 and 3150 K is analyzed as shown in Table 4-13. Those temperatures correspond to the corium superheats of 50 and 300 K respectively. The results show that the energetics of EVSE in terms of pressure impulse increases with the corium temperature; 168.27 and 216.69 kPa-s for 50 K and 300 K superheat of corium, respectively. However, it also shows that the peak pressures for three cases; minimum, base, and maximum, are in a similar range of approximately 57-67 MPa. It indicates that the increase of thermal contents of corium enhances the explosion pressure peaks and profiles.

4.5.3.2. Corium Ejection Velocity Effects

The corium ejection velocity influences directly to the mixing phase of steam explosion process,

mainly to corium jet breakup. In general, jet breakup length depends on the Froude number, and the ratio of density ratios between jet and coolant as shown in Eq. (4-2) below, showing the linear increase of the jet breakup length with the jet velocity,

$$\frac{\mathrm{L}}{D_j} \propto \left(\frac{\rho_j}{\rho_c}\right)^{0.5} (Fr)^{0.5} \quad \text{(Eq. 4.2)}$$

where,

$$\mathrm{Fr} \propto \frac{V_j^2}{gD_j} \quad \text{(Eq. 4.3)}$$

The jet breakup diameter during the breakup process in the TEXAS-V code is calculated based upon the Weber number in terms of the relative velocity between jet and coolant. Therefore, as the corium jet velocity increases the jet breakup occurs in a deeper penetration length and the diameter of fragmented jet becomes exponentially decreases. This process provides the finer mixing particle diameters, resulting more energetic steam explosion. Table 4-14 shows that the peak pressures and the impulses of steam explosion increases from 48.3 to 83.4 MPa and from 83.1 to 181.9 kPa-s as the jet velocity increases from 1 to 6 m/s.

4.5.3.3. Corium Jet Diameter

The corium jet diameter directly influences on the corium mass participation in the EVSE process. For the computational stability, the ARIY parameter is adjusted. As shown in Table 4-15, the effect of the corium jet diameter significantly influences on the EVSE energetics. For the jet diameter of 0.1 and 0.6, the resulting peak pressures and the maximum impulses become 12.34 to 86.42 MPa and 35.74 to 250.12 kPa-s.

4.5.3.4. Corium Temperature

Table 4-16 shows that the effect of coolant temperature, the degree of water subcooling in the cavity show no significant effect on the EVSE energetics comparing to those from other parameters.

4.6. Corium Material Effects on EVSE Energetics

It is worth noting that the analysis was performed with the 1-D TEXAS-V code that potentially provides the conservative maximum energetics for the given initial and boundary conditions. In addition, the TEXAS-V model has been validated for the KROTOS-alumina tests that provided the high energetics. However, recent experimental results with corium suggested that the energetics of steam explosion with the corium composition is very limited. To verify this issue, TEXAS-V analysis for the recent TROI TS-4 test has been performed. As shown in Figure 4-10 the TEXAS-V significantly over-predict the corium experimental pressure, explain the conservatism associated with the present TEXAS-V model and results of potential conservatism in the reactor case analysis like in this work.

4.7. Reactor Cavity Structural Integrity Assessment

4.7.1. Introduction